日放腫会誌 J Jpn Soc Ther Radiol Oncol 20: 119-125, 2008

非侵襲的呼吸同期照射に向けた腹壁運動と肺腫瘍運動との相関解析

中村 光宏[*1]，成田 雄一郎[*1]，松尾 幸憲[*1]，檜林 正流[*1]，中田 学[*2]，
矢野 慎輔[*2]，澤田 晃[*1]，溝脇 尚志[*1]，永田 靖[*3]，平岡 眞寛[*1]

CORRELATIVE ANALYSIS OF ABDOMINAL MOTION WITH LUNG TUMOR MOTION FOR NON-INVASIVE RESPIRATORY GATED RADIOTHERAPY

Mitsuhiro NAKAMURA[*1], Yuichiro NARITA[*1], Yukinori MATSUO[*1],
Masaru NARABAYASHI[*1], Manabu NAKATA[*2], Shinsuke YANO[*2], Akira SAWADA[*1],
Takashi MIZOWAKI[*1], Yasushi NAGATA[*3], Masahiro HIRAOKA[*1]

(Received 17 April 2008, accepted 4 August 2008)

Abstract: Purpose: The purposes of this study were to assess the correlation between lung tumor motion and the abdominal motion, and to estimate the position mismatch as the difference between the abdominal motion trace used to the predicted lung tumor position and the measured lung tumor position.
Methods and Materials: Eleven patients who underwent stereotactic body radiotherapy between December 2006 and March 2008 were included in this study. Of all the patients, 6 were studied over 3 days under an internal review board approved protocol. Breathing synchronized fluoroscopy was performed under free breathing. Measurements of the anterior-posterior abdominal skin surface displacement by the Real-time Positioning Management System (Varian Medical Systems, Inc., Palo Alto, CA) were correlated to simultaneously acquired X-ray fluoroscopy (Acuity; Varian Medical Systems, Inc.) measurements of superior-inferior tumor displacement. The lung tumor motion was analytically detected by a template matching algorithm after image processing. To evaluate the tumor-abdominal motion phase relationship, a cross-correlation was calculated of the time-synchronized tumor motion and the abdominal motion. By comparing the predicted lung tumor position in which phase difference was corrected to the measured lung tumor position, the position mismatch was computed.
Results: The correlation coefficients between the lung tumor motion and abdominal motion ranged 0.89 from 0.97 and more reproducible from day to day. A hysteresis curve was observed due to phase difference between the lung tumor motion and abdominal motion. The average of the position mismatch was up to 1.78 mm.
Conclusion: Even if the correlation coefficients between the abdominal motion and the tumor motion were high for most cases, there were some differences between the predicted lung tumor position and the measured lung tumor position.

Key words: Respiratory gated radiotherapy, Lung tumor motion, Respiration surrogate

はじめに

放射線治療における照射技術の高度化に伴い，体内臓器の呼吸性移動に対する関心がますます高まりつつある中，American Association of Physicists in Medicineは，呼吸性移動への対応に関する報告書を発表した[1]．これによると，X線透視や四次元CT，シネMRIなどで，腫瘍の呼吸性移動を評価した結果，場所によっては30mmに及ぶと報告されている．

呼吸性移動を伴う腫瘍に対して放射線治療を行う場合，腫瘍の移動範囲をすべて含んだ内的標的体積を設定し，更にセットアップマージンを加味した計画標的体積(以下，PTV)に対して照射野を設定する照射法(以下，motion inclusive法)が一般的である．呼吸性移動が小さい場合はmotion inclusive法でも，正常組織に対する線量を低く抑えつつ，PTVへの線量を確保することが可能であるが，呼吸性移動が大きい腫瘍に対してmotion inclusive法を適応すると，PTVサイズが結果的に大きくなり，正常組織に対する不必要な線量が多くなる．われわれは肺定位放射線治療において，腫瘍の呼吸性移動が大きい症例に対して，呼吸性移動抑制を目的とした腹部圧迫板を使用しているが，抑制効果が小さい場合や呼吸機能が悪いことが原因で腹部圧迫板を使用できない症例を経験している．

腫瘍に対する線量を確保しつつ，正常組織に対する線量を低減させる照射方法の一つとして，呼吸同期照射法がある．呼吸同期照射法は腫瘍に対して呼吸周期中の特定の位

[*1]京都大学大学院医学研究科放射線腫瘍学・画像応用治療学(〒606-8507 京都市左京区聖護院川原町54)(Department of Radiation Oncology and Image-applied Therapy, Kyoto University Graduate School of Medicine)(54 Shogoin-Kawaharacho, Sakyo-ku, Kyoto 606-8507, JAPAN)，[*2]京都大学医学部附属病院放射線部(Clinical Radiology Service, Kyoto University Hospital)，[*3]広島大学病院放射線治療部(Division of Radiation Oncology, Hiroshima University Hospital)

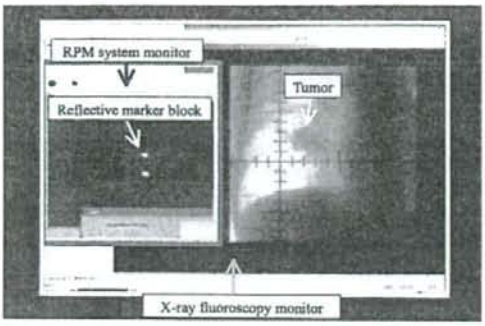

Fig. 1 A parallel display between RPM system monitor representing abdominal wall motion using a reflective marker block, and a chest fluoroscopic image from the anterior of a patient.

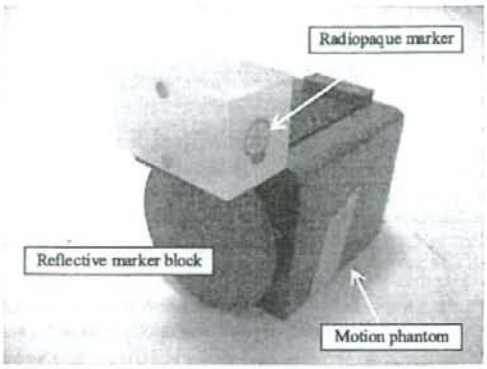

Fig. 2 A motion phantom and a reflective marker block.

相もしくは位置にタイミングを合わせて照射を行う方法であり，1980年代後半に日本で開始されて以来[2]，現在では多くの施設で施行されている[1]．この照射方法は，腫瘍近傍に留置された放射線不透過マーカー等を直接観測しながら照射を行う侵襲的呼吸同期照射と，腫瘍の呼吸性移動の代替信号として腹壁変位量や換気流量等を用いる非侵襲的呼吸同期照射に大別される[1]．

代替信号と体内臓器もしくは放射線不透過マーカーの相関性に関しては，多くの報告がなされている[3)-7)]．Mageras[3]やVedamら[4]は，腹壁変位量と横隔膜の頭尾方向の変位量の間に良好な位相の相関関係があると報告した．肺腫瘍に対して非侵襲的呼吸同期照射を実施する場合，横隔膜ではなく，肺腫瘍を直接評価する方が望ましいと考える．Ahn[5]やHoisakら[6]は，腹壁変位量もしくは換気流量と肺腫瘍の頭尾方向の変位量(以下，肺腫瘍変位量)を計測し，これらの間に大きな位相ずれが生じる場合があると報告した．高精度に非侵襲的呼吸同期照射を行うためには，代替信号が予測する腫瘍位置と実際の腫瘍位置との間に生じるずれ量(以下，腫瘍位置ずれ量)を考慮する必要があると考える．Ionascuら[7]は腫瘍近傍に留置された放射線不透過マーカー位置と腹壁変位量が予測した肺腫瘍位置のずれは頭尾方向で2.5mm以上に及ぶ場合があると報告したが，放射線不透過マーカーを使用せずに，腫瘍位置ずれ量を測定した報告はなされていない．

当院では呼吸性移動を伴う腫瘍に対して，腹壁変位量に基づく非侵襲的呼吸同期照射の臨床適用を検討している．本研究の目的は放射線不透過マーカーを使用せずに，X線シミュレーターで計測した肺腫瘍変位量と商用の呼吸同期照射システムで取得した腹壁変位量との位相相関性を評価し，腫瘍位置ずれ量を算出することである．

方　法

1. 使用機器

肺腫瘍変位量の観測にはX線シミュレーター(Acuity; Varian Medical Systems, Inc., Palo Alto, CA)を使用し，肺腫瘍変位量の代替信号である腹壁変位量の取得にはReal-time Positioning Managementシステム(以下，RPMシステム; Varian Medical Systems, Inc.)を使用した．RPMシステムでは，対象に貼付した赤外線反射マーカーからの反射赤外線をCCDカメラが受光し，30 frame/secで赤外線反射マーカー位置を検出した．

2. 画像収集及び解析方法

RPMシステム画面とX線透視画面の時間軸を一致させるために，Local Area Network(以下，LAN)を介したWindows XPのリモートデスクトップ機能を利用し，RPMシステム画面とX線透視画面を並列に表示した(Fig. 1)．LANのデータ転送速度の理論最大値は1Gbpsであり，また，X線シミュレーターとRPMシステムのみのネットワーク構成とすることで，信号遅延を抑制した．X線シミュレーターに接続したDVDドライブで，並列表示したRPMシステム画面とX線透視画面をDVDメディアに録画した．次に，DVDメディアに保存した時系列画像に対して，最大吸気位相，最大呼気位相及び中間位相における肺腫瘍テンプレートを用いたテンプレートマッチングにより，肺腫瘍位置を検出し，その頭尾方向の変位量を解析した．

1)信号遅延検証

LANを介したリモートデスクトップ機能の利用による信号遅延を検証した．RPMシステム付属の動体ファントムに設置した赤外線反射マーカー上に放射線不透過マーカーを貼付し，上下運動させた(Fig. 2)．X線シミュレーターのガントリーを90度回転させた状態で，約60秒間撮影(画像取得間隔：0.03秒，取得静止画像枚数：約1,800枚)し，リモートデスクトップ機能を利用して，RPMシステム画面とX線透視画面の並列表示画像を取得した．取得画像から二値化処理により，赤外線反射マーカー位置と放射線不透過マーカー位置を検出し，これらの相関係数を算出した．

Table 1 Individual patient characteristics

Patient	Age	Sex	Location	Multiple days
1	78	M	RLL	Yes
2	58	M	RML	No
3	77	M	RLL	Yes
4	62	F	LLL	Yes
5	81	M	LLL	No
6	81	M	LUL	Yes
7	77	F	RLL	Yes
8	78	M	RLL	No
9	78	M	RML	Yes
10	80	M	LLL	No
11	74	F	RLL	No

Abbreviations: M, male; F, female; RLL, right lower lobe; RML, right middle lobe; LLL, left lower lobe; LUL, left upper lobe.

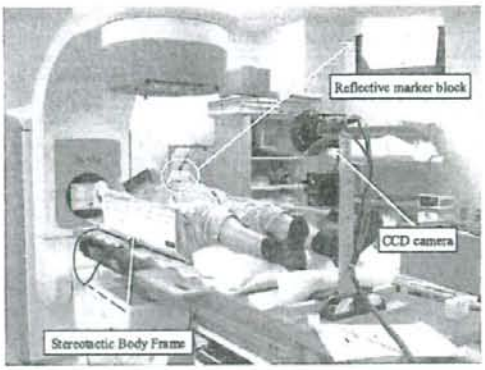

Fig. 3 Typical patient setup. A reflective marker block placed midway between the patient's xiphoid process and umbilicus was used in the recording of the respiration signal.

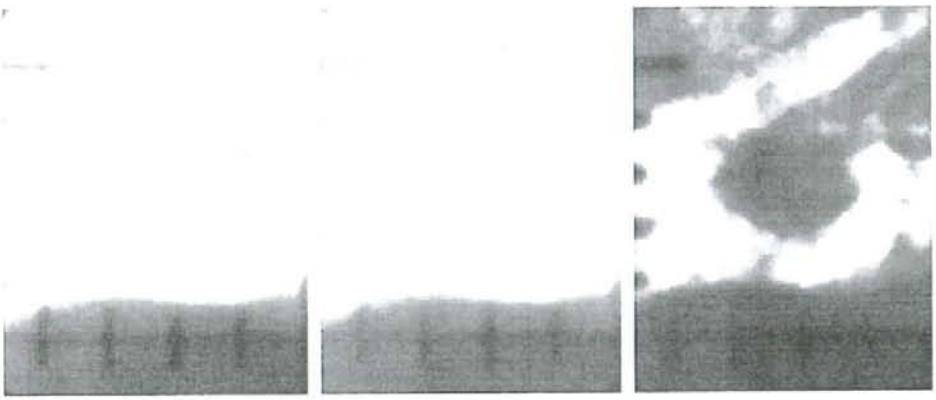

Fig. 4 An example of image processing.
(a) An original image.
(b) The median filter was used to reduce noise in images.
(c) The contrast between tumor and background was enhanced.

a | b | c

2)臨床画像

対象症例

2006年12月から2008年 3 月までの間に，当院で肺定位放射線治療を施行した症例のうち，X線透視画像上で肺腫瘍の同定が可能であり，その変位量が頭尾方向に平均で 8mm 以上と，複数の放射線腫瘍医によって判断された11症例を対象とした(Table 1)．

治療計画時に患者の固定具(stereotactic body frame; Elekta Corp., Stockholm, Sweden)を作成後，赤外線反射マーカーを患者の剣状突起と臍部の中心付近に貼付した(Fig. 3)．次に，X線シミュレーターのガントリー角度を 0 度とし，自由呼吸下で約60秒間撮影(画像取得間隔：0.03秒，取得静止画像枚数：約1,800枚)し，リモートデスクトップ機能を利用して，RPMシステム画面とX線透視画面の並列表示画像を取得した．尚，対象症例のうち 6 症例は倫理審査委員会の承認の下，治療期間中の 2 日間においても測定を行った．1 回目測定(以下，Session 1)から 2 回目測定(以下，Session 2)までは少なくとも 5 日間以上開いており，3 回目測定(以下，Session 3)までの期間は最大で10日間であった．

画像処理及び解析

RPMシステム画像を二値化処理し，赤外線反射マーカー位置を検出した．次に，X線透視画像に対してカーネルサイズが 3×3 のメディアンフィルターを適用し，平滑化した．更に，肺腫瘍検出範囲内のピクセル値ヒストグラムの平坦化を行い，肺腫瘍とバックグラウンドのコントラストを強調した(Fig. 4)．肺腫瘍の動体追跡にはテンプレートマッ

Table 2 Tumor-abdominal motion correlation coefficients over all measurement sessions

Patient	Session 1	Session 2	Session 3
1	0.97	0.97	0.97
2	0.89	n/a	n/a
3	0.96	0.96	0.95
4	0.97	0.96	0.94
5	0.96	n/a	n/a
6	0.93	0.95	0.94
7	0.89	0.96	0.93
8	0.96	n/a	n/a
9	0.93	0.97	0.97
10	0.96	n/a	n/a
11	0.89	n/a	n/a

Abbreviation: n/a, not available (patient did not participate in this measurement session).

Table 3 Phase difference between superior-inferior tumor motion and anterior-posterior abdominal motion

Patient	Session 1	Session 2	Session 3
1	0.03	0.03	0.00
2	0.33	n/a	n/a
3	0.10	0.13	0.10
4	0.10	0.13	0.07
5	0.13	n/a	n/a
6	0.07	0.07	0.07
7	0.13	0.10	0.13
8	0.00	n/a	n/a
9	0.03	0.10	0.10
10	0.00	n/a	n/a
11	0.23	n/a	n/a

Abbreviation: n/a, not available (patient did not participate in this measurement session).
Notes: A positive value indicates that the lung tumor motion is lagging behind abdominal motion. All values are in seconds.

チングを使用した．肺腫瘍の呼吸性移動や変形及び骨構造との重なりによる誤検出を抑えるため，テンプレートには呼吸周期が安定している最大吸気位相，最大呼気位相，及び，その中間呼吸位相における 3 種類の画像を用意した．これにより，X線透視画像中の任意の呼吸位相における肺腫瘍検出能が向上するように工夫した．各テンプレート画像とX線透視画像の非類似度 $\{D_k,\ k\in\{end\text{-}in,\ end\text{-}ex,\ mid\}\}$ を式(1)～(3)で評価し，算出した非類似度が最小となる位置 (x^*, y^*) を肺腫瘍位置とした(式(4))．

$$D_{end\text{-}in}(x,y)=\sum_{i=0}^{M-1}\sum_{j=0}^{N-1}\left\{f(x+i,y+j)-g_{end\text{-}in}(i,j)\right\}^2 \quad (1)$$

$$D_{end\text{-}ex}(x,y)=\sum_{i=0}^{M-1}\sum_{j=0}^{N-1}\left\{f(x+i,y+j)-g_{end\text{-}ex}(i,j)\right\}^2 \quad (2)$$

$$D_{mid}(x,y)=\sum_{i=0}^{M-1}\sum_{j=0}^{N-1}\left\{f(x+i,y+j)-g_{mid}(i,j)\right\}^2 \quad (3)$$

$$(x^*,y^*)=\arg\min_{(x,y)\in R}\left(D_{end\text{-}in}(x,y),D_{end\text{-}ex}(x,y),D_{mid}(x,y)\right) \quad (4)$$

ここで，MとNはそれぞれテンプレート画像の縦と横のピクセル数，$f(x, y)$〔ただし，$(x, y)\in R$であり，肺腫瘍検出範囲内をRとした〕は，X線透視画像のピクセル位置(x, y)におけるピクセル値，$g_{end\text{-}in}(i,j)$，$g_{end\text{-}ex}(i,j)$ 及び $g_{mid}(i,j)$ は，それぞれ最大吸気位相，最大呼気位相及び中間位相のテンプレート画像のピクセル値を表す．

肺腫瘍位置の検出後，腹壁変位量と肺腫瘍変位量の位相に対する相関係数及び位相ずれを算出した．得られた相関の有意性を検定するために，無相関検定を行った．また，相関係数が最も 1 に近づくように位相ずれを補正し，そこで得られた回帰直線を基に腹壁変位量が予測する肺腫瘍位置を求め，測定した肺腫瘍位置と比較することで，腫瘍位置ずれ量の平均値及び99%信頼区間を算出した．

結　果

1. 信号遅延検証

赤外線反射マーカー位置と放射線不透過マーカー位置の位相相関係数はほぼ 1 となり，LANを介したリモートデスクトップ機能を利用することによる信号遅延は無視できるほど小さかった．

2. 位相相関性

臨床画像における位相相関性及び位相ずれの解析結果を，それぞれTable 2 及びTable 3 に示す．複数日間にわたって測定を行った症例の日々の変動(以下，日間変動)は比較的安定していた(Table 2, Session 1-3)．相関係数の無相関検定を行った結果，すべてのSessionで$p<0.0001$であった．

呼吸パターンは必ずしも規則正しくはなく，測定中に呼吸パターンが不規則な症例も見られた．それらの中で，特徴的な相関図及び腹壁変位量と肺腫瘍変位量の時系列グラフをFig. 5，Fig. 6 及びFig. 7 に示す．患者 1 のSession 2 における時系列グラフでは，測定開始直後から15秒後まで，患者の呼吸が呼気位相で中断しており(Fig. 5a)，相関図中の呼気位相に集合体が形成された(Fig. 5b)．60秒間の測定においても，呼吸パターンは不規則であったが，相関係数の絶対値は0.97であった．患者 2 のSession 1 における時系列グラフでは，肺腫瘍変位量と腹壁変位量の間に位相ずれが観測された(Fig. 6a)．相関係数の絶対値は0.89であったが，その相関図はヒステリシス曲線を描いていた(Fig. 6b)．この場合，腫瘍位置ずれは顕著であった．患者 9 のSession 2 における時系列グラフでは，測定開始30秒後に深呼吸をしていた(Fig. 7a)．このとき，相関図中の軌跡は大きくはずれ，ループを描いていた(Fig. 7b)が，測定時間内における相関係数の絶対値は0.97であった．

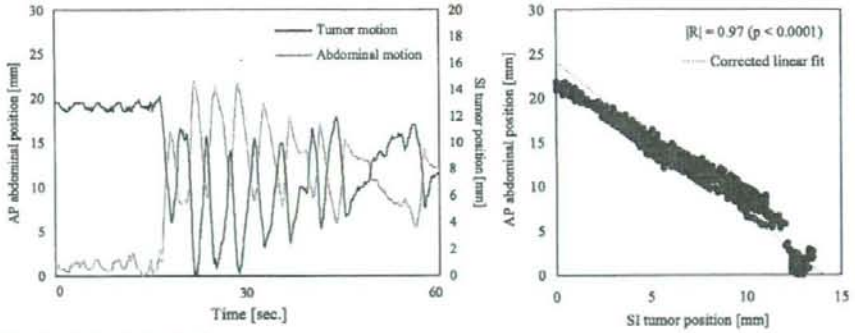

Fig. 5 Patient 1, Session 2
(a) Superior-inferior tumor motion and anterior-posterior abdominal motion as a function of time.
(b) Superior-inferior tumor position as a function of anterior-posterior abdominal position. Even if the respiratory pattern is irregular, the correlation coefficient is high (|R|=0.97; p<0.0001).

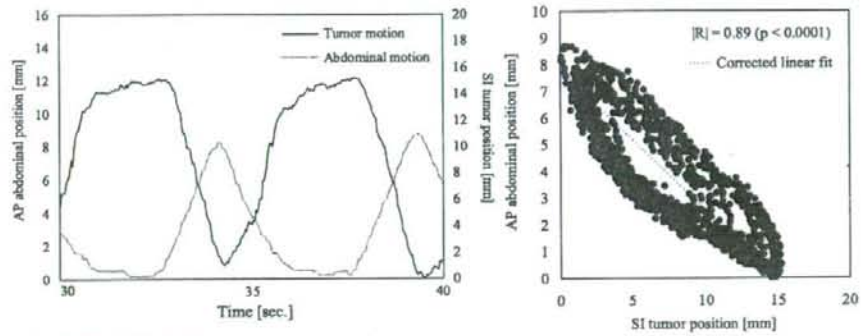

Fig. 6 Patient 2, Session 1
(a) Superior-inferior tumor motion and anterior-posterior abdominal motion as a function of time.
(b) Superior-inferior tumor position as a function of anterior-posterior abdominal position. The loop caused by respiratory phase lag between abdominal and tumor motion was observed (|R|=0.89; p<0.0001).

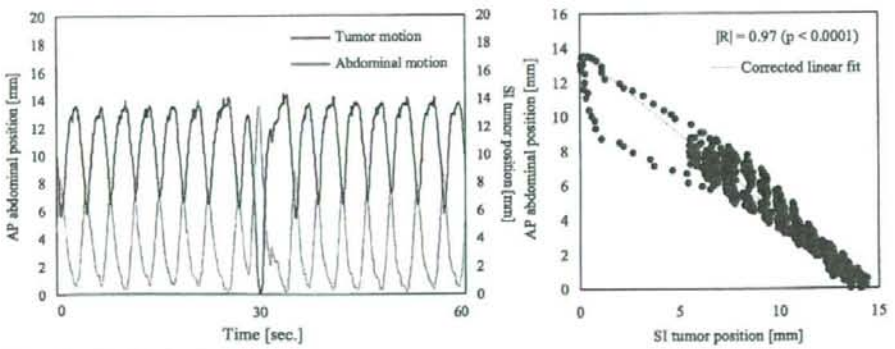

Fig. 7 Patient 9, Session 2
(a) Superior-inferior tumor motion and anterior-posterior abdominal motion as a function of time.
(b) Superior-inferior tumor position as a function of anterior-posterior abdominal position. The patient breathed deeply after 30 sec (|R|=0.97; p<0.0001).

Table 4 The position mismatch between the predicted tumor position and the measured tumor position

Patient	Session 1			Session 2			Session 3		
	Mean	99% C.I.		Mean	99% C.I.		Mean	99% C.I.	
		Lower	Upper		Lower	Upper		Lower	Upper
1	0.49	0.47	0.52	0.71	0.68	0.73	0.61	0.59	0.64
2	1.78	1.71	1.85		n/a			n/a	
3	1.70	1.63	1.77	0.88	0.85	0.92	1.00	0.95	1.06
4	1.21	1.15	1.26	1.26	1.18	1.33	0.61	0.58	0.64
5	1.42	1.35	1.49		n/a			n/a	
6	0.44	0.42	0.46	0.73	0.70	0.76	0.67	0.64	0.70
7	0.84	0.80	0.88	0.53	0.50	0.55	0.86	0.83	0.90
8	0.46	0.44	0.48		n/a			n/a	
9	0.77	0.73	0.81	0.45	0.42	0.48	0.69	0.66	0.71
10	1.73	1.66	1.81		n/a			n/a	
11	1.55	1.46	1.64		n/a			n/a	

Abbreviations: C.I., confidence interval; n/a, not available (patient did not participate in this measurement session).
Notes: All values are in millimeters.

3. 腫瘍位置ずれ量

全症例において，腹壁変位量が予測した肺腫瘍位置と測定した肺腫瘍位置にずれが認められた(Table 4)．Table 4の平均値及び99%信頼区間幅から，腫瘍位置ずれ量の日内及び日間変動は一定ではないことが示された．同一患者間の位相相関係数が同じであっても，腫瘍位置ずれ量は異なる値を示した．深呼吸をした場合，腫瘍位置ずれ量は最大で5mmに及ぶことがわかった(Fig. 7b)．

考　察

本研究では，LANを介したリモートデスクトップ機能を利用し，RPMシステムで取得した腹壁変位量とX線シミュレーターから取得した肺腫瘍変位量の時間軸を同期させて解析することを試みた．信号遅延検証結果及び画像取得間隔が0.03秒であることから，信号遅延は0.03秒未満であり，赤外線反射マーカー位置及び放射線不透過マーカー位置の時系列データの時間軸は非常に高い精度で一致していた．

複数日にわたる測定では，患者のセットアップ，赤外線反射マーカーの貼付位置，皮膚のたるみや胃内の充満度の違い等で，CCDカメラと赤外線反射マーカーの幾何学的位置関係が異なる．しかし，腹壁変位量と肺腫瘍変位量の位相相関の日間変動が小さいことから，実臨床で想定される赤外線反射マーカーとCCDカメラの幾何学的位置関係の違いによる位相の相関性への影響は非常に小さいと考えられる．Ahnら[5]は，体表面に直接貼付した放射線不透過マーカーと腫瘍もしくは横隔膜との位相相関性を解析した結果，相関係数の平均値±標準偏差は0.77±0.12であり，特に下肺野の腫瘍や横隔膜と放射線不透過マーカーとの間には強い相関があったと結論付けた．本研究で得られた位相相関係数は0.95±0.03と，Ahnら[5]の結果よりも高かった．

Hoisakら[6]は独自のシステムを構築し，これを用いて肺腫瘍変位量と腹壁変位量との位相相関について検証した結果，相関係数は0.39から0.98と，幅広く分布していることを示した．位相相関が悪い症例では，肺腫瘍変位量と腹壁変位量で最大0.65秒の位相ずれが生じており，その相関図は位相ずれに起因するヒステリシス曲線を描いていた．本研究でも，例えば患者2のSession 1における位相相関係数は高い値を示していたが，肺腫瘍変位量と腹壁変位量の間に0.33秒の位相ずれが生じていた(Fig. 6b)．位相ずれが発生する原因の一つとして，呼吸方式の差異が考えられる．呼吸方式には，横隔膜や腹筋を使う腹式呼吸と肋間筋を使う胸式呼吸の二種類がある．胸式呼吸では，吸気時において胸郭が広がると共に肺腫瘍が動き出し，続いて腹壁が動くため，腹壁変位量と肺腫瘍変位量の位相ずれが生じると考えられる．一方，腹式呼吸では，横隔膜及び腹壁が動き出すと同時に肺に空気が取り込まれ，それに伴って肺腫瘍も動き出すため，腹壁変位量と肺腫瘍変位量の相関は良好であると推測する．腹壁変位量を肺腫瘍変位量の代替信号として用いる場合，腹式呼吸へ誘導できれば，腹壁変位量と肺腫瘍変位量の相関が向上し，非侵襲的呼吸同期照射の高精度化が図れると考える．また，呼吸パターンが不規則な患者に対して呼吸コーチングを適用することにより，呼吸パターンの再現性が向上するだけでなく[3), 8)-11)]，呼吸同期照射の効率が向上すると報告されており[10), 11)]，非侵襲的呼吸同期照射のスループット向上との相乗効果も期待できる．

代替信号が正確に腫瘍の呼吸性移動を表現していない状態で非侵襲的呼吸同期照射を行うと，腫瘍に対して過小線量のまま治療が完遂する恐れがある．本研究では放射線不透過マーカーを使わずに腫瘍位置ずれ量が求まることを実証し，Ionascuら[7]と同様の結果を得た．位相に対して高い相関係数を示しても，腹壁変位量が予測した肺腫瘍位置と測定した肺腫瘍位置にはずれが生じており，この値を無視できない症例も見られた．これらのずれ量を実臨床に反映させるには，腫瘍位置ずれ量を保証するマージンの設定もしくは呼吸同期幅の拡大等の対応が必要と考える．ただし，今回得られた腫瘍位置ずれ量は60秒の測定時間から得られた値であり，1回当たりの治療時間が60秒よりも長い場合や腹壁変位量のベースラインシフト等の影響で，腫瘍位置ずれ量が更に大きくなる可能性も考えられる．

結　論

赤外線反射マーカーと肺腫瘍の動きを同時に計測及び解析できる方法を考案し，これらの位相相関性及び腹壁変位量が予測した肺腫瘍位置と測定した肺腫瘍位置のずれ量を解析した．多くの症例で，腹壁変位量と肺腫瘍変位量との位相の相関関係は良好であり，これらの日間変動も安定していた．しかし，腹壁変位量が予測した肺腫瘍位置と測定した肺腫瘍位置の間にずれが生じていた．

謝辞：本研究の遂行にあたり，ご協力を賜りました京都大学医学部附属病院放射線治療部門の皆様に，誌面を借りて深謝申し上げます．

本研究の一部は，平成20年度科学研究費補助金基盤研究(S)(課題番号：20229009)の一部として実施された．

文　献

1) Keall PJ, Mageras GS, Balter JM, et al.: The management of respiratory motion in radiation oncology report of AAPM Task Group 76. *Med Phys* **33**: 3874-3900, 2006.
2) Ohara K, Okumura T, Akisada M, et al.: Irradiation synchronized with respiration gate. *Int J Radiat Oncol Biol Phys* **17**: 853-857, 1989.
3) Mageras GS, Yorke E, Rosenzweig K, et al.: Fluoroscopic evaluation of diaphragmatic motion reduction with a respiratory gated radiotherapy system. *J Appl Clin Med Phys* **2**: 191-200, 2001.
4) Vedam SS, Kini VR, Keall PJ, et al.: Quantifying the predictability of diaphragm motion during respiration with a noninvasive external marker. *Med Phys* **30**: 505-513, 2003.
5) Ahn S, Yi B, Suh Y, et al.: A feasibility study on the prediction of tumour location in the lung from skin motion. *Br J Radiol* **77**: 588-596, 2004.
6) Hoisak JD, Sixel KE, Tirona PC, et al.: Correlation of lung tumor motion with external surrogate indicators of respiration. *Int J Radiat Oncol Biol Phys* **60**: 1298-1306, 2004.
7) Ionascu D, Jiang SB, Nishioka S, et al.: Internal-external correlation investigations of respiratory induced motion of lung tumors. *Med Phys* **34**: 3893-3903, 2007.
8) Kini VR, Vedam SS, Keall PJ, et al.: Patient training in respiratory-gated radiotherapy. *Med Dosim* **28**: 7-11, 2003.
9) Kubo HD and Wang L: Introduction of audio gating to further reduce organ motion in breathing synchronized radiotherapy. *Med Phys* **29**: 345-350, 2002.
10) George R, Chung TD, Vedam SS, et al.: Audio-visual biofeedback for respiratory-gated radiotherapy: Impact of audio instruction and audio-visual biofeedback on respiratory-gated radiotherapy. *Int J Radiat Oncol Biol Phys* **65**: 924-933, 2006.
11) Nelson C, Starkschall G, Balter P, et al.: Respiration-correlated treatment delivery using feedback-guided breathhold: A technical study. *Med Phys* **32**: 175-181, 2005.

要旨：【目的】本研究の目的は，商用の呼吸同期照射システムで得た背腹方向の腹壁変位量とX線シミュレーターで観測した頭尾方向の肺腫瘍変位量の位相相関性を評価し，腹壁変位量が予測した腫瘍位置と測定した腫瘍位置のずれ量(以下，腫瘍位置ずれ量)を算出することであった．【方法】2006年12月から2008年3月までの間に，当院で肺定位放射線治療を施行した11症例を対象とした．そのうち6症例は倫理審査委員会の承認の下，3日間にわたって測定を行った．Real-time Positioning Managementシステム(Varian Medical Systems, Inc., Palo Alto, CA)で計測した腹壁変位量の画面と肺腫瘍変位量が投影されたX線シミュレーター(Acuity; Varian Medical Systems, Inc.)の画面を並列に表示し，自由呼吸下で60秒間計測した．取得した並列画像に対して画像処理を行った後，テンプレートマッチングで肺腫瘍の位置を検出した．腹壁変位量と肺腫瘍変位量から位相相関性を評価した．また，位相ずれを補正した回帰直線を用いて，腹壁運動が予測した肺腫瘍位置を求め，これと測定した肺腫瘍位置を比較することで，腫瘍位置ずれ量を算出した．【結果】相関係数の絶対値は0.89から0.97の範囲内にあり，これらの日々の変動も安定していた．腹壁変位量と肺腫瘍変位量の位相ずれが原因で生じるヒステリシス曲線を描く症例も存在した．腫瘍位置ずれ量の平均値は最大で1.78mmであった．【結論】多くの症例で，腹壁変位量と肺腫瘍変位量との位相相関性は良好であったが，腹壁変位量が予測した肺腫瘍位置と測定した肺腫瘍位置の間にずれが生じていた．

Int. J. Radiation Oncology Biol. Phys., Vol. 72, No. 2, pp. 398–403, 2008

0360-3016/08/$–see front matter

doi:10.1016/j.ijrobp.2008.01.002

CLINICAL INVESTIGATION **Lung**

STEREOTACTIC BODY RADIOTHERAPY FOR OLIGOMETASTATIC LUNG TUMORS

YOSHIKI NORIHISA, M.D.,* YASUSHI NAGATA, M.D., PH.D.,* KENJI TAKAYAMA, M.D.,* YUKINORI MATSUO, M.D., PH.D.,* TAKASHI SAKAMOTO, M.D.,† MASATO SAKAMOTO, M.D.,‡ TAKASHI MIZOWAKI, M.D., PH.D.,* SHINSUKE YANO, B.S.,* AND MASAHIRO HIRAOKA, M.D., PH.D.*

*Department of Radiation Oncology and Image-Applied Therapy, Kyoto University Graduate School of Medicine, Kyoto, Japan; †Department of Radiation Oncology, Kumamoto University Graduate School of Medical Sciences, Kumamoto, Japan; and ‡Department of Radiology, Japanese Red Cross Society Wakayama Medical Center, Wakayama, Japan

Purpose: Since 1998, we have treated primary and oligometastatic lung tumors with stereotactic body radiotherapy (SBRT). The term "oligometastasis" is used to indicate a small number of metastases limited to an organ. We evaluated our clinical experience of SBRT for oligometastatic lung tumors.

Methods and Materials: A total of 34 patients with oligometastatic lung tumors were included in this study. The primary involved organs were the lung ($n = 15$), colorectum ($n = 9$), head and neck ($n = 5$), kidney ($n = 3$), breast ($n = 1$), and bone ($n = 1$). Five to seven, noncoplanar, static 6-MV photon beams were used to deliver 48 Gy ($n = 18$) or 60 Gy ($n = 16$) at the isocenter, with 12 Gy/fraction within 4–18 days (median, 12 days).

Results: The overall survival rate, local relapse-free rate, and progression-free rate at 2 years was 84.3%, 90.0%, and 34.8%, respectively. No local progression was observed in tumors irradiated with 60 Gy. SBRT-related pulmonary toxicities were observed in 4 (12%) Grade 2 cases and 1 (3%) Grade 3 case. Patients with a longer disease-free interval had a greater overall survival rate.

Conclusion: The clinical result of SBRT for oligometastatic lung tumors in our institute was comparable to that after surgical metastasectomy; thus, SBRT could be an effective treatment of pulmonary oligometastases. © **2008 Elsevier Inc.**

Stereotactic body radiotherapy, Metastatic lung tumor, Pulmonary metastases, Oligometastases.

INTRODUCTION

Stereotactic irradiation, stereotactic radiosurgery, and stereotactic radiotherapy are standard therapeutic techniques for intracranial tumors. With the introduction of three-dimensional localization techniques using a localizing frame of reference, hypofractionated irradiation using a stereotactic technique has been applied to extracranial tumors. Stereotactic body radiotherapy (SBRT) represents one of those treatments, and SBRT has been used in many institutes (1–9) mainly to irradiate lung or liver cancer.

Recently, patients with oligometastases, that is, a small number of metastatic lesions limited to an organ, have been considered candidates for curative treatment because long-term survival can be expected (10–13); therefore, surgical resection is the standard choice for patients with oligometastatic lung cancer. Since the effectiveness of SBRT for primary lung cancer was reported (5, 7, 14–17), awareness has been growing of SBRT as an effective option for curative treatment of lung tumors. In 1998, we began using SBRT for both primary and oligometastatic lung tumors. In this study, we retrospectively analyzed our experience with SBRT outcomes for oligometastatic lung tumors and reviewed the published data.

METHODS AND MATERIALS

Patient and tumor characteristics

The eligibility criteria of SBRT for oligometastatic lung tumor were as follows: *(1)* one or two pulmonary metastases, *(2)* tumor diameter ≤4 cm, *(3)* locally controlled primary tumor, and *(4)* no other metastatic sites. Of the patients treated between December 1998 and December 2004, 34 with oligometastatic lung tumors were included in this study. The primary involved organs were the lung ($n = 15$), colorectum ($n = 9$), head and neck ($n = 5$), kidney ($n = 3$), breast ($n = 1$), and bone ($n = 1$). Of these 34 patients, 25 were treated for

Reprint requests to: Yasushi Nagata, M.D., Ph.D., Department of Radiation Oncology and Image-Applied Therapy, Kyoto University Graduate School of Medicine, 54 Shogoin-Kawahara-Cho, Sakyo-Ku, Kyoto 606-8507, Japan. Tel: (+81) 75-751-3762; Fax: (+81) 75-751-3418; E-mail: nag@kuhp.kyoto-u.ac.jp

Supported by Grant-in-Aid H18-014 from the Ministry of Health, Labour and Welfare, Japan and Grant-in-Aid 18390333 from the Ministry of Education and Science, Japan.

Presented in part at the 46th Annual Meeting of the American Society for Therapeutic Radiology and Oncology (ASTRO), Atlanta, GA, October 3–7, 2004.

Conflict of interest: none.

Received Feb 5, 2007, and in revised form Dec 27, 2007. Accepted for publication Jan 3, 2008.

a single pulmonary nodule and 9 for two lesions. The histologic diagnosis of the primary disease was adenocarcinoma in 22, squamous cell carcinoma in 5, renal cell carcinoma in 3, adenoid cystic carcinoma in 2, pleomorphic carcinoma in 1, and osteosarcoma in 1 patient. Lung metastases were diagnosed clinically according to repeated thoracic computed tomography (CT) findings. Most patients had previously undergone surgical resection and chemotherapy for their primary cancer. Adjuvant oral chemotherapy regimens after SBRT were allowed. The patient characteristics are given in Table 1.

SBRT procedure

We used a combined X-ray and CT simulator—an integrated system using the same couch for the X-ray and CT simulators (Shimadzu, Kyoto, Japan). The patients were fixed in the stereotactic body frame (ELEKTA AB, Stockholm, Sweden) while CT scanning was performed with a slow scan time (4 s/slice).

Three-dimensional RT planning was performed using a treatment-planning machine (CADPLAN, version 3.1, and Eclipse, version 7.1, Varian Medical Systems, Palo Alto, CA). The internal target volume (ITV) was delineated on the CT images, considering the tumor motion assessed by X-ray fluoroscopy, and then the essential margins—planning target volume (PTV) margin and leaf margins—were added to the ITV (18, 19). We added 5 mm to the ITV for the PTV margin and another 5 mm from the contour of the PTV to the edge of the multileaf collimator for penumbra; thus, typically, a 10-mm margin was used between the contour of the ITV and the edge of the multileaf collimator. We used five to seven noncoplanar, static 6-MV photon beams and irradiated 12 Gy in each fraction at the isocenter. The patients received four or five fractions; therefore, the total dose was 48 Gy or 60 Gy at the isocenter within 4–18 days (median, 12 days).

Because we experienced several local failures with 48 Gy, the prescribed dose was escalated to 60 Gy from January 2001. However, the dose for metastases from primary lung cancer was maintained at 48 Gy because of difficulties in distinguishing a second primary lung cancer from a metastatic lesion and because the 5-year local relapse-free rate of 95% using this dose (16) was satisfactory. Also, the general pulmonary function was better in patients with metastatic lung cancer than in those with primary lung cancer. With the exception of patients with poor pulmonary function, a total dose of 60 Gy was prescribed to patients with a primary cancer other than lung cancer.

Table 1. Patient characteristics

Characteristic	Value
Patients (*n*)	34
Gender (*n*)	
Male	22
Female	12
Age (y)	
Range	30–80
Median	71
Performance status	
0	23
1	9
2	2
3–5	0
Primary tumor	
Lung	15
Colorectum	9
Head and neck	5
Kidney (renal cell carcinoma)	3
Bone (osteosarcoma)	1
Breast	1

Evaluation

The local response was assessed using the Response Evaluation Criteria in Solid Tumors and categorized into four types: *(1)* the disappearance of all target lesions (complete response), *(2)* at least a 30% decrease in the sum of the longest diameter of the target lesions (partial response), *(3)* a response ranging from a 30% decrease to a 20% increase in the sum of the longest diameter of the target lesions (stable disease), and *(4)* a ≥20% increase in the sum of the longest diameter of the target lesions (progressive disease). Because of the presence of consolidation with unclear margins around the tumor (20), it can be difficult to distinguish between tumor regrowth and radiation-induced injury; such cases were categorized as stable disease until apparent tumor regrowth was detected by careful and appropriate clinical observation for several months.

Survival was calculated from the first day of RT to the last day of follow-up. For overall survival, lost patients with clinically progressive disease and those with the terminal stage of disease were censored as dead. Adverse events were classified according to the Common Terminology Criteria for Adverse Events, version 3.

Statistical calculations were performed using Prism, version 4, software (GraphPad Software, San Diego, CA). The survival rates were analyzed using the Kaplan-Meier method, and differences in their distributions were evaluated using the log–rank test.

RESULTS

The study population comprised 22 men and 12 women, with median age of 71 years (range, 30–80 years). Of these 34 patients, 17 received 48 Gy in four fractions and 16 received 60 Gy in five fractions. One patient received 48 Gy in five fractions because of poor pulmonary function that necessitated a reduction in the fractional dose. The overall treatment time was 4–14 days (median, 12 days), except for

Table 2. Treatment results

Variable	Value
Tumor total (*n*)	43
Tumor diameter (*n*)	
<15 mm	17
≥15 but ≤30 mm	22
>30 mm	4
Prescribed dose (Gy)	
48	18
60	16
Overall treatment time (d)	
Range	4–18
Median	12
Follow-up period (mo)	
Range	10–80
Median	27

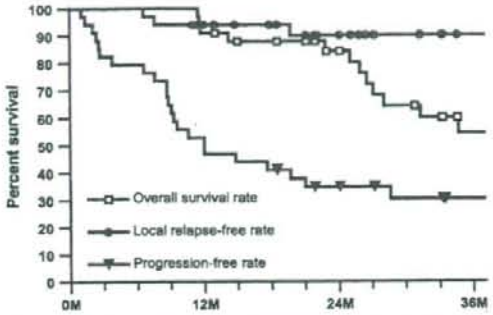

Fig. 1. Overall survival, local relapse-free survival, and progression-free survival rates after stereotactic body radiotherapy for oligometastatic lung cancer.

1 patient, for whom it was 18 days. The median follow-up period was 27 months (range, 10–80 months; Table 2).

Response

The overall survival rate, local relapse-free rate, and progression-free rate at 2 years was 84.3%, 90.0%, and 34.8%, respectively (Fig. 1). The numbers of patients with a complete response, partial response, stable disease, and progressive disease was 5, 8, 18, and 3, respectively. No statistically significant difference was found between those receiving 60 Gy and those receiving 48 Gy in terms of overall survival (p = 0.192; Fig. 2a); however, a marginally significant difference was observed between those receiving 60 Gy and 48 Gy in local progression-free survival (p = 0.078; Fig. 2b). No local progression was observed in tumors irradiated to 60 Gy, but three had local progression at 48 Gy. No differences were found in overall survival between patients with metastases from lung cancer and those with metastases from other cancers (p = 0.75).

Patterns of failure

Disease progression was observed in 23 patients (Table 3). Regrowth of the target lesions of SBRT was observed in 3 patients and recurrence of the primary lesion in 2. New metastatic lesions were observed in 19 patients. New intrapulmonary metastases were observed in 9 patients, and mediastinal or hilar regional lymph nodal metastases developed in 6. Distant metastases were observed in 3 patients: the adrenal gland in 2 and the liver in 1. One patient was diagnosed with progressive disease because of elevations of carcinoembryonic antigen and underwent chemotherapy.

Toxicity

The adverse events resulting from SBRT were classified using the Common Terminology Criteria for Adverse Events, version 3 (Table 4). Pulmonary toxicity was observed as cough, hemosputum, dyspnea, pleural effusion, and radiographic changes and was Grade 1 in 23 patients (68%) and Grade 2 in 4 (12%). One patient required oxygen

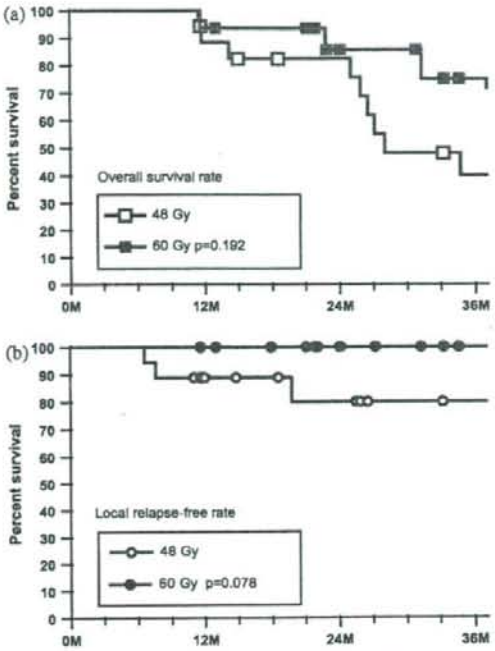

Fig. 2. (a) Overall survival rates of patients treated with 48 Gy and 60 Gy. (b) Local relapse-free rates of patients treated with 48 Gy and 60 Gy. Difference was marginally significant (p = 0.078).

supplementation for bacterial pneumonia 18 months after SBRT and was considered to have Grade 3 pulmonary toxicity. The symptoms of most patients were mild and did not interfere with their activities of daily living. Grade 1 skin toxicity with faint erythema or pigmentation with or without symptoms was observed in 6 patients (17%). One patient had a skin ulcer at the site of the reirradiated field, contralateral to the site of SBRT, and was cured with conservative treatment. Musculoskeletal adverse events were

Table 3. Patterns of disease progression

Pattern	*n*
New pulmonary metastasis	9
Regional lymph node metastasis	6
Local regrowth of target lesion of SBRT	3
Recurrence of primary lesion	2
Adrenal gland metastasis	2
Liver metastasis	1
Tumor marker elevation without any apparent recurrence	1

Abbreviation: SBRT = stereotactic body radiotherapy.

Of 34 patients, disease progression observed in 23 patients; 1 patient had regrowth at site of SBRT and liver metastasis simultaneously.

Table 4. Toxicity

Toxicity	Grade 0	1	2	3
Pulmonary	6	23	4	1
Skin	27	6	1	0
Pain	27	6	0	0
Musculoskeletal	32	2	0	0
Cardiac general (pericardial effusion)	32	2	0	0
Hepatobiliary	33	1	0	0

Total number of patients was 34.

observed in 2 patients (6%): bone fracture of the rib and musculitis of the chest wall. With these dermatologic or musculoskeletal complications of the thoracic wall, mild pain was observed in 6 patients (17%). Grade 1 pericardial effusion and temporal liver dysfunction were observed in 1 patient (3%) each. Most adverse events remained at Grade 1. No adverse effects of the spinal cord, great vessels, or esophagus were observed.

Prognostic factors

We also analyzed the survival differences stratified by the disease-free interval (DFI), previous chemotherapy, previous thoracic surgery, performance status, nodule size (sum of longer diameters), and number of targets. Except for DFI, no significant differences were observed. We stratified patients into three groups according to the DFI; <1 year, >1 year but <3 years, and >3 years (Fig. 3). Patients with DFI >3 years had significantly greater overall survival (p = 0.02) among the three groups. However, other factors showed negative results, which might suggest a limitation of this small group study.

DISCUSSION

Our clinical standard dose fractionation of SBRT for primary lung cancer was 48 Gy in four fractions. For metastatic lung cancer, we escalated the dose to 60 Gy because three local failures occurred with the 48-Gy dose. At last follow-up, 60 Gy appears to have been well tolerated by the patients with lung metastases. No local progression occurred with the 60-Gy dose. The difference between 48 and 60 Gy was not statistically significant in the survival rate, but was marginally significant (p = 0.078) in the local progression rate. The incidence of Grade 1 and 2 pulmonary toxicity was comparable between the two doses, with 13 (72%) and 2 (11%) at 48 Gy and 10 (63%) and 2 (13%) at 60 Gy, respectively. Dose escalation from 48 to 60 Gy increased the local control rate without increasing the incidence or severity of pulmonary toxicity.

Several reports have been published regarding the outcomes of SBRT for primary or metastatic lung tumors. Table 5 lists the survival outcomes after SBRT for pulmonary metastases in these reports. Onimaru *et al.* (8) and Wulf

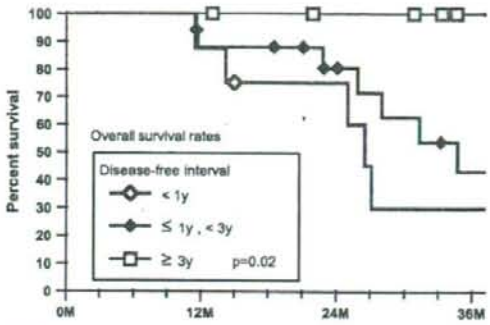

Fig. 3. Overall survival rates stratified by disease-free interval (p = 0.02).

(14) reported overall survival rates of 49% and 33% at 2 years. Lee *et al.* (7) did not report the actuarial 2-year survival rate, although we calculated the crude survival rate to be 68% from data in their summary table. In the present study, it was 84%. The biologically effective dose, assuming the α/β ratio to be 10 (BED_{10}), in the present study was 105.6 Gy and 132.0 Gy for 48 Gy in four fractions and 60 Gy in five fractions, respectively. Onishi *et al.* (15) concluded that a BED_{10} of >100 Gy at the isocenter is preferable for the treatment of primary lung cancer to achieve a better overall survival rate. The BED_{10} of SBRT for pulmonary metastases ranged from 70 to 162 Gy, and the survival rates at 2 years ranged from 33% to 84% (Table 5).

An important aspect when discussing these results is the difference in treatment planning. One is the dose prescription point. We prescribed the dose to the isocenter. In contrast, some institutes prescribed to the margin of the PTV. Second is the PTV margin. The PTV margin differs depending on the setup accuracy at each institution. Third is the PTV contour. Contouring of the PTVs would reflect a difference in CT scanning: CT scanning with free breathing vs. breath holding and slow vs. fast scan times. Fourth is the dose calculation algorithm, including the inhomogeneity correction. Differences in the dose calculation algorithm would affect the marginal dose, particularly in treatment planning for lung tumors. Thus, we prescribed the dose to the isocenter to avoid unintended dose variations. Recently, more accurate dose calculation has become common, and adoption of a prescription with respect to the PTV is also worth considering, if a standard method has been established.

Surgical pulmonary metastasectomy has been recognized as a potentially curative treatment, particularly for patients without other metastases. Our published data review revealed that the 5-year survival rate for these patients was 26–40% (21–30) (Table 6). According to the International Registry of Lung Metastases, with >5,000 cases, surgical resection for metastatic lung tumor can result in long-term survival (21). In the International Registry of Lung

Table 5. SBRT for pulmonary metastases

Investigator	Primary tumor (*n*)	Patients (*n*)	Prescription	BED_{10} @ IC	Target	2-y Survival rate (%)
Lee *et al.* (7), 2003	Lung 5, liver 3, esophagus 2, trachea 2	19	30 Gy/3 Fr to 40 Gy/4 Fr		CTV: GTV + 5 mm	68*
		12	30 Gy/3 Fr (median 90% @ PTV margin)	70†	PTV: CTV + 5–10 mm	
		7	40 Gy/4 Fr (median 90% @ PTV margin)	94†		
Onimaru *et al.* (8), 2003	Lung 6, kidney 6, breast 2	20	48 Gy/8 Fr to 60 Gy/8 Fr		ITV	49
		15	48 Gy/8 Fr @ IC	76.8	PTV: ITV + 5–10 mm	
		5	60 Gy/8 Fr @ IC	105.0		
Wulf *et al.* (14), 2004	Lung 23, breast 5, colorectum 4, kidney 4, sarcoma 4	51	26 Gy/1 Fr to 37.5 Gy/3 Fr		CTV: GTV + 2–3 mm	33
		25	26 Gy/1 Fr (80% @ PTV margin)	138†	PTV: CTV+ 5–10 mm	
		12	30 Gy/3 Fr (100% @ PTV margin, 150% @ IC)	112.5		
		5	36 Gy/3 Fr (100% @ PTV margin, 150% @ IC)	151.2		
		9	37.5 Gy/3 Fr (100% @ PTV margin, 150% @ IC)	161.7		
Present study	Lung 15, colorectum 9, head and neck 5, kidney 3	34	48 Gy/4 Fr to 60 Gy/5 Fr		ITV	84
		18	48 Gy/4 Fr @ IC	105.6	PTV: ITV + 5 mm	
		16	60 Gy/5 Fr @ IC	132.0		

Abbreviations: SBRT = stereotactic body radiotherapy; BED_{10} = biologically effective dose ($\alpha/\beta = 10$); IC = isocenter; Fr = fractions; CTV = clinical target volume; GTV = gross tumor volume; PTV = planning target volume; ITV = internal target volume.

* Calculated from patient summary table.

† Estimations according to their marginal doses.

Metastases study, with the exclusion of the apparently favorable tumors (*i.e.*, germ cell and Wilms tumors), the survival outcome at 2 years was approximately 70%. In our study, the overall survival rate at 2 years was 84%. Thus, SBRT appears to have the potential to cure, similar to that of surgical metastasectomy.

Table 6. Results of metastasectomy

Investigator	Year	Primary cancer	Patients (n)	5-y Survival rate (%)
IRLM (21)	1997	Various	4,572	36
		Epithelial tumor	1,984	
		Sarcoma	1,917	
		Germ cell tumor	318	
		Melanoma	282	
		Other	70	
van Rens *et al.* (23)	2001	Lung	121	26
Saito *et al.* (25) (KCOG)	2002	Colorectum	165	40
Pfannschmidt *et al.* (27)	2003	Colorectum	167	32

Abbreviations: IRLM = International Registry of Lung Metastases; KCOG = Kansai Clinical Oncology Group.

The International Registry of Lung Metastases also analyzed prognostic factors. They found that a DFI of ≥36 months, a single metastasis, and germ cell or Wilms tumor as the primary tumor were factors resulting in a good prognosis. In our study, a longer DFI of >3 years was also a good prognostic factor. They also showed that the difference in relative risk was not substantial for those with common epithelial cancers such as those of the bowel, breast, head and neck, and kidney. In our study, no significant difference was found in overall survival between those with metastases from lung cancer and those with metastases from other sites. For selected patients with pulmonary oligometastases, survival after SBRT might not be affected by the primary disease.

CONCLUSION

The optimal regimen of SBRT for pulmonary metastasis has not yet been determined: 60 Gy was well tolerable and was superior to 48 Gy for local control at 2 years. SBRT for oligometastatic lung tumors was comparable to surgical metastasectomy with regard to the 2-year overall survival rate. SBRT could be an effective treatment for oligometastatic lung tumors.

REFERENCES

1. Uematsu M, Shioda A, Tahara K, *et al.* Focal, high dose, and fractionated modified stereotactic radiation therapy for lung carcinoma patients: A preliminary experience. *Cancer* 1998;82: 1062–1070.
2. Nakagawa K, Aoki Y, Tago M, *et al.* Megavoltage CT-assisted stereotactic radiosurgery for thoracic tumors: Original research in the treatment of thoracic neoplasms. *Int J Radiat Oncol Biol Phys* 2000;48:449–457.
3. Wulf J, Hadinger U, Oppitz U, *et al.* Stereotactic radiotherapy of extracranial targets: CT-simulation and accuracy of treatment in the stereotactic body frame. *Radiother Oncol* 2000;57:225–236.
4. Hara R, Itami J, Kondo T, *et al.* Stereotactic single high dose irradiation of lung tumors under respiratory gating. *Radiother Oncol* 2002;63:159–163.
5. Nagata Y, Negoro Y, Aoki T, *et al.* Clinical outcomes of 3D conformal hypofractionated single high-dose radiotherapy for one or two lung tumors using a stereotactic body frame. *Int J Radiat Oncol Biol Phys* 2002;52:1041–1046.
6. Hof H, Herfarth KK, Munter M, *et al.* Stereotactic single-dose radiotherapy of stage I non-small-cell lung cancer (NSCLC). *Int J Radiat Oncol Biol Phys* 2003;56:335–341.
7. Lee SW, Choi EK, Park HJ, *et al.* Stereotactic body frame based fractionated radiosurgery on consecutive days for primary or metastatic tumors in the lung. *Lung Cancer* 2003;40:309–315.
8. Onimaru R, Shirato H, Shimizu S, *et al.* Tolerance of organs at risk in small-volume, hypofractionated, image-guided radiotherapy for primary and metastatic lung cancers. *Int J Radiat Oncol Biol Phys* 2003;56:126–135.
9. Onishi H, Kuriyama K, Komiyama T, *et al.* A new irradiation system for lung cancer combining linear accelerator, computed tomography, patient self-breath-holding, and patient-directed beam-control without respiratory monitoring devices. *Int J Radiat Oncol Biol Phys* 2003;56:14–20.
10. Singh D, Yi WS, Brasacchio RA, *et al.* Is there a favorable subset of patients with prostate cancer who develop oligometastases? *Int J Radiat Oncol Biol Phys* 2004;58:3–10.
11. Kavanagh BD, McGarry RC, Timmerman RD. Extracranial radiosurgery (stereotactic body radiation therapy) for oligometastases. *Semin Radiat Oncol* 2006;16:77–84.
12. Yang JC, Abad J, Sherry R. Treatment of oligometastases after successful immunotherapy. *Semin Radiat Oncol* 2006;16: 131–135.
13. Rubin P, Brasacchio R, Katz A. Solitary metastases: Illusion versus reality. *Semin Radiat Oncol* 2006;16:120–130.
14. Wulf J, Haedinger U, Oppitz U, *et al.* Stereotactic radiotherapy for primary lung cancer and pulmonary metastases: A noninvasive treatment approach in medically inoperable patients. *Int J Radiat Oncol Biol Phys* 2004;60:186–196.
15. Onishi H, Araki T, Shirato H, *et al.* Stereotactic hypofractionated high-dose irradiation for stage I nonsmall cell lung carcinoma: Clinical outcomes in 245 subjects in a Japanese multiinstitutional study. *Cancer* 2004;101:1623–1631.
16. Nagata Y, Takayama K, Matsuo Y, *et al.* Clinical outcomes of a phase I/II study of 48 Gy of stereotactic body radiotherapy in 4 fractions for primary lung cancer using a stereotactic body frame. *Int J Radiat Oncol Biol Phys* 2005;63: 1427–1431.
17. Zimmermann FB, Geinitz H, Schill S, *et al.* Stereotactic hypofractionated radiation therapy for stage I non-small cell lung cancer. *Lung Cancer* 2005;48:107–114.
18. Negoro Y, Nagata Y, Aoki T, *et al.* The effectiveness of an immobilization device in conformal radiotherapy for lung tumor: Reduction of respiratory tumor movement and evaluation of the daily setup accuracy. *Int J Radiat Oncol Biol Phys* 2001; 50:889–898.
19. Takayama K, Nagata Y, Negoro Y, *et al.* Treatment planning of stereotactic radiotherapy for solitary lung tumor. *Int J Radiat Oncol Biol Phys* 2005;61:1565–1571.
20. Aoki T, Nagata Y, Negoro Y, *et al.* Evaluation of lung injury after three-dimensional conformal stereotactic radiation therapy for solitary lung tumors: CT appearance. *Radiology* 2004;230: 101–108.
21. The International Registry of Lung Metastases. Long-term results of lung metastasectomy: Prognostic analyses based on 5206 cases. *J Thorac Cardiovasc Surg* 1997;113:37–49.
22. Asaph JW, Keppel JF, Handy JR Jr., *et al.* Surgery for second lung cancers. *Chest* 2000;118:1621–1625.
23. van Rens MT, Zanen P, de la Riviere AB, *et al.* Survival after resection of metachronous non-small cell lung cancer in 127 patients. *Ann Thorac Surg* 2001;71:309–313.
24. Sakamoto T, Tsubota N, Iwanaga K, *et al.* Pulmonary resection for metastases from colorectal cancer. *Chest* 2001;119: 1069–1072.
25. Saito Y, Omiya H, Kohno K, *et al.* Pulmonary metastasectomy for 165 patients with colorectal carcinoma: A prognostic assessment. *J Thorac Cardiovasc Surg* 2002;124: 1007–1013.
26. Rena O, Casadio C, Viano F, *et al.* Pulmonary resection for metastases from colorectal cancer: factors influencing prognosis: Twenty-year experience. *Eur J Cardiothorac Surg* 2002; 21:906–912.
27. Pfannschmidt J, Muley T, Hoffmann H, *et al.* Prognostic factors and survival after complete resection of pulmonary metastases from colorectal carcinoma: experiences in 167 patients. *J Thorac Cardiovasc Surg* 2003;126:732–739.
28. Inoue M, Ohta M, Iuchi K, *et al.* Benefits of surgery for patients with pulmonary metastases from colorectal carcinoma. *Ann Thorac Surg* 2004;78:238–244.
29. Monteiro A, Arce N, Bernardo J, *et al.* Surgical resection of lung metastases from epithelial tumors. *Ann Thorac Surg* 2004;77:431–437.
30. Kondo H, Okumura T, Ohde Y, *et al.* Surgical treatment for metastatic malignancies—Pulmonary metastasis: Indications and outcomes. *Int J Clin Oncol* 2005;10:81–85.

IOP PUBLISHING PHYSICS IN MEDICINE AND BIOLOGY

Phys. Med. Biol. 53 (2008) 2413–2423 doi:10.1088/0031-9155/53/9/013

Time-dependent cell disintegration kinetics in lung tumors after irradiation

Alexei V Chvetsov[1], Jatinder J Palta[1] and Yasushi Nagata[2]

[1] Department of Radiation Oncology, University of Florida, Gainesville, FL, USA
[2] Department of Therapeutic Radiology and Oncology, Kyoto University, Kyoto, Japan

E-mail: chvetsov@ufl.edu

Received 27 January 2008, in final form 17 March 2008
Published 17 April 2008
Online at stacks.iop.org/PMB/53/2413

Abstract

We study the time-dependent disintegration kinetics of tumor cells that did not survive radiotherapy treatment. To evaluate the cell disintegration rate after irradiation, we studied the volume changes of solitary lung tumors after stereotactic radiotherapy. The analysis is performed using two approximations: (1) tumor volume is a linear function of the total cell number in the tumor and (2) the cell disintegration rate is governed by the exponential decay with constant risk, which is defined by the initial cell number and a half-life $T_{1/2}$. The half-life $T_{1/2}$ is determined using the least-squares fit to the clinical data on lung tumor size variation with time after stereotactic radiotherapy. We show that the tumor volume variation after stereotactic radiotherapy of solitary lung tumors can be approximated by an exponential function. A small constant component in the volume variation does not change with time; however, this component may be the residual irregular density due to radiation fibrosis and was, therefore, subtracted from the total volume variation in our computations. Using computerized fitting of the exponent function to the clinical data for selected patients, we have determined that the average half-life $T_{1/2}$ of cell disintegration is 28.2 days for squamous cell carcinoma and 72.4 days for adenocarcinoma. This model is needed for simulating the tumor volume variation during radiotherapy, which may be important for time-dependent treatment planning of proton therapy that is sensitive to density variations.

1. Introduction

The goal of this paper is to show that the time-dependent disintegration of tumor cells which do not survive radiotherapy can be described using a simple analytical function. These cells are supposed to be lethally damaged by radiation with the probability described, for instance, by the LQ-model; however, they exist in some intact form and contribute to the tumor volume

0031-9155/08/092413+11$30.00 Printed in the UK

even though they are not able to proliferate (Fowler 1989, Hall and Giaccia 2006). We assume that these cells disintegrate at the first or subsequent division and their debris is removed from the tumor. This mechanism called mitotic death is a common form of cell death after irradiation; however, the probability of other disintegration mechanisms like apoptosis can also be included in our model (Hall and Giaccia 2006). The time-dependent kinetics which we apply to the population of lethally damaged cell has also been successfully used for the population of neurons with inherited degenerations (Clarke *et al* 2000). The neuron population with inherited degenerations is very similar to the lethally damaged tumor cells because they do not proliferate and their death initiated by a random event. For the analysis of this time-dependent cell kinetics, we utilized a clinical study on the volumetric changes of solitary lung tumors after stereotactic body radiotherapy (Aoki *et al* 2004).

The disintegration model of lethally damaged cells can be used in more complicated models which describe complete tumor cell kinetics during radiation therapy. This kinetics which includes both living and lethally damaged cells is implemented, for instance, in the computer models developed by Borkenstein *et al* (2004) and Dionysiou *et al* (2004). Potentially, these models can predict tumor volume during fractionated radiotherapy which can be important for time-dependent treatment planning because the tumor volume variation causes density variations which, in turn, can affect the prescribed dose distributions. During the last few years, several clinical studies have been published on tumor volume variation *in vivo* during fractionated radiotherapy. The data in these studies have been obtained using integrated 3D imaging techniques such as CT/linear accelerator system or tomotherapy (Barker *et al* 2004, Kupelian *et al* 2005, Siker *et al* 2006). Similar studies on tumor volume variation have been done using conventional CT scanners for treatment modalities where the integrated 3D imaging was not available, for instance proton therapy (Bucci *et al* 2007). The acquired data indicate that the physiological geometry changes in tumors and normal tissues between dose fractions can affect the dose distributions during fractionated radiotherapy, with an apparent maximum effect for lung and head and neck cancers. The research on tumor volume variation is important for intensity-modulated radiation therapy (IMRT), which provides sharp dose fall-off around the tumor (Mohan *et al* 2005). Emergent proton therapy is even more sensitive to the physiological changes because of the limited range of proton beams (Engelsman and Kooy 2005, Bucci *et al* 2007).

New models for tumor volume variation have been developed which can describe anatomical changes during fractionated radiotherapy (Seibert *et al* 2007, Chao *et al* 2007). These models are based on deformable image registration techniques or database analysis; however, they do not utilize the underlying radiobiological mechanisms. Therefore, these models cannot explain many phenomena which have been observed in tumor volume variation measurements. They lack predictive power because they do not utilize radiobiological principles. We believe that radiobiological models are necessary to explain these observed phenomena and predict tumor shrinkage based on radiobiological principles.

In the radiobiological modeling for radiotherapy treatment planning research has been primarily dedicated to developing effective dose fractionation schedules, models for tumor control probability (TCP) and normal tissue complication probability (NTCP) (Moiseenko *et al* 2005, Stewart and Li 2007). Less attention has been paid to the models for volume and mass variations during radiotherapy because it was likely not assumed that these changes could significantly affect the dose distributions and treatment outcomes. The cell loss mechanisms have been studied for growing tumors to explain the difference between the potential doubling time and volume doubling time (Fowler 1991); however, the problems of quantitative evaluation of dosimetry due to volume and mass variation in treatment planning have not been addressed. Circumstances have changed recently with the invention and widespread use

of effective imaging technologies which allow monitoring of human tumors *in vivo* (Barker *et al* 2004, Kupelian *et al* 2005, Siker *et al* 2006). Volumetric radiobiological tumor response to irradiation with X-rays has been studied in animal experiments (Tannock and Howes 1973, Bernheim *et al* 1977, Spang-Thomsen *et al* 1981). The obtained data have been important for understanding the radiobiological mechanisms responsible for tumor regression; however, they cannot be applied directly to the human tumors irradiated *in vivo*. The data required for *in vivo* verification of tumor volume modeling are available now due to 3D integrated imaging technologies for monitoring the tumor volume variation during radiotherapy treatment.

In this paper, we propose a simple radiobiological model for cell disintegration kinetics after radiation damage. We believe that this model can motivate further development of the computationally efficient and practical models that describe cell kinetics and tumor-volume changes during radiotherapy. These models can potentially be used to improve time-dependent treatment planning.

2. Methods

2.1. Cell survival, death and disintegration

Irradiation of the tumor cell population with dose D causes the death of a fraction of cells. The survival process of living cells can be described using the linear-quadratic (LQ) model which is given by

$$S = \exp(-\alpha D - \beta D^2), \tag{1}$$

where α and β are the parameters of the survival model (Fowler 1989, Hall and Giaccia 2006). The survival curve S defines the relative number of cells which survive; therefore, the relative number of cells which are lethally damaged by radiation is given by $1-S$. Usually, the number of surviving clonogens is studied in treatment planning because they finally define the TCP. In this paper, we study the clonogens which did not survive irradiation because we believe that the kinetics of these clonogens defines the tumor volume variation during radiotherapy. The clonogens which are lethally damaged by radiation do not disappear instantly. They contribute to the tumor volume for a period of time until they disintegrate and their debris is removed from the tumor. This kinetics of cell loss can help us to evaluate the time-dependent tumor volume variation which, in turn, can affect the dose distributions.

It is difficult to derive the cell disintegration kinetics using the data on tumor-volume variation during radiotherapy because the tumor volume is defined by the kinetics of proliferating and damaged cells. However, after radiotherapy, we can assume that the entire cell population did not survive irradiation and is lethally damaged; therefore, we have only one cell subpopulation which is much easier to model. The clinical data on the tumor-volume variation after radiotherapy are available, for instance, for solitary lung tumors treated with stereotactic body radiotherapy (Aoki *et al* 2004).

2.2. Cell disintegration model

It is usually assumed that a cell damaged by radiation disintegrates at the first or a subsequent division after radiation damage at the dose levels used in therapy. During the time from radiation damage to disintegration, the damaged cells contribute to the tumor volume even though they are not able to proliferate. We assume that the cell disintegration rate is proportional to the number of intact damaged cells; therefore, we can write the following

differential equation for the time-dependent number of damaged cells:

$$\frac{dN(t)}{dt} = -\mu(t)N(t). \tag{2}$$

We further introduce an approximation of constant disintegration risk which assumes that the disintegration constant is time independent $\mu(t) = \mu_0$. Equation (2) with $\mu(t) = \mu_0$ has an analytical exponential decay solution which is given by

$$N(t) = N(t_0)\exp(-\mu_0 t). \tag{3}$$

where $N(t_0)$ is the number of dead intact cells at the initial time t_0. This approach is similar to the mathematical formalism used by Clarke *et al* (2000) to describe the time-dependent kinetics of cell death in inherited neuronal degenerations.

Similar to the formula for radioactive decay, we introduce a parameter called half-life for the biological decay of the damaged cell population. The half-life is defined as the time required for the number of damaged cells to decay to half of their initial value. The half-life of the damaged cell population is related to the decay constant μ_0 as

$$T_{1/2} = \frac{\ln 2}{\mu_0}. \tag{4}$$

The key problem for practical applications of this approach is to evaluate the half-life of the population of damaged cells. We have already mentioned that damaged cells disintegrate at the first attempted division; therefore, the disintegration rate may be associated with the proliferation rate because both parameters are related to the cell cycle. It is convenient to assume that the half-life $T_{1/2}$ is linearly related to the potential doubling time T_{pot} as

$$T_{1/2} = bT_{pot}, \qquad b > \ln 2. \tag{5}$$

If we take into account that the cell disintegration happens at the first or subsequent division, we can further establish that $T_{1/2} > \ln 2T_{pot}$, which allows for the parameter $b > \ln 2$. We have utilized here the relationship $T_{1/2} = \ln 2T_a$ between the half-life $T_{1/2}$ and the mean life T_a. Obviously, we have $T_a = T_{pot}$ if all damaged cells would disintegrate at the first division. For more detailed evaluation of the half-life $T_{1/2}$, we have to study the variation with time of a large population of damaged cells *in vivo*. The large population of damaged cells can be found, for instance, at the end of radiotherapy treatment where the entire population of cancer cells is assumed to have not survived irradiation.

2.3. Tumor volume simulation

One of the possible ways to study the kinetics of cell disintegration is to evaluate the tumor volume after radiotherapy because we can assume that the entire tumor cell population did not survive radiotherapy. This is a relatively simple mathematical problem because we have to evaluate only one cell subpopulation damaged by radiation and unable to proliferate. However, to evaluate the kinetics of cell disintegration based on the volumetric measurements, we have to assume a linear relationship between the tumor volume $V(t)$ and the cell number $N(t)$:

$$V(t) = vN(t), \tag{6}$$

where v is a constant which includes the cell volume and the volume of the related intercellular space. Experiments with animal irradiation indicate that the mean cell concentration in tumors can be a function of delivered radiation dose and time. Therefore, the gross changes in the tumor volume after irradiation are not always a reliable indicator of microscopic changes in the cell number. However, the experimental data of Tannock and Howes indicate that the mean cell concentration returns to the near-normal values after a limited time between 1 and 7 days

(Tannock and Howes 1973). For instance, Tannock and Howes have measured a 75% reduction in the mean cell concentration after 6 Gy with 1 day of recovery time and a 50% reduction in the mean cell concentration after 30 Gy with 7 days of recovery time. Therefore, we believe that the linear relationship between the cell number and the tumor volume is a reasonable approximation for tumor volume simulation in the clinical study analyzed in this paper. In this clinical study, tumors have been monitored during several months after radiotherapy.

3. Results

3.1. Clinical data analysis

To validate the exponential model and determine decay parameters, we used the clinical data on tumor size variation after stereotactic body radiotherapy published by Aoki *et al* (2004). This clinical study includes analysis of shrinkage of solitary lung tumors in 31 patients after administering a total dose of 48 Gy in four fractions using conformal stereotactic radiation therapy. Taking into account the survival fraction given by equation (1), we can assume that the entire cell population tumors did not survive the radiotherapy for the majority of patients at this dose; therefore, the tumor volume variation after radiotherapy should be defined by the disintegration and removal of damaged cells which are not able to proliferate. This is probably true for most of the patients because tumor control was not obtained in only two cases.

The tumor size variation with time was determined by taking CT images after radiotherapy. The relative variation of tumor size as a function of time is shown in figure 1(a) for three representative cases. Additionally, we show in figure 1(a) an exponent function with $T_{1/2} =$ 21 days. We see that the exponent function approximates the general trend in tumor size variation with time. However, the difference is that the exponent function approaches zero and the tumor volume variation approaches some constant value.

We note that the tumor size in the clinical study has been measured using the largest transversal cross section A of the tumor. To evaluate the tumor volume variation, we computed the relative change of value $AA^{1/2}$ which presents the relative volumetric change under the assumption of uniform tumor shrinkage. The relative change of the value $AA^{1/2}$ is shown in figure 1(b). We see that the constant component was reduced when the data have been recalculated to the volumetric tumor change. This small constant component in the volume variation does not change with time; therefore, this component may be due to residual irregular density as radiation fibrosis and was, therefore, subtracted from volume variation in our computations.

3.2. Evaluation of half-life and average life

To determine the half-life $T_{1/2}$ of exponential decay, we performed a computerized fitting of the exponent function to the clinical data for seven adenocarcinoma and seven squamous cell carcinoma (SCC) patients. The clinical study of Aoki *et al* includes 15 adenocarcinoma cases, 9 SCC cases, 4 metastasis cases, 2 unknown cases and 1 small cell carcinoma case. We have separated the adenocarcinoma and SCC cases and excluded all other cases. The tumor shrinkage was observed in all adenocarcinoma and SCC patients; however, not all of them had enough tumor size measurements to perform a reasonable fitting. Therefore, the patients for the fitting have been selected based on the number and density of tumor measurements available for each case. One of our selection criteria was the availability of at least three tumor measurements for each patient and at least one tumor measurement within the first 4 months after treatment.

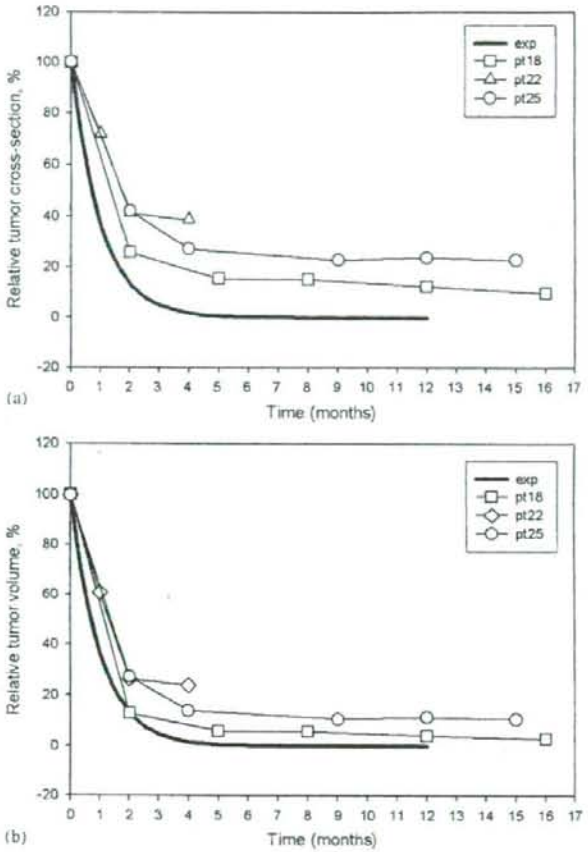

Figure 1. Comparison of relative tumor size variation after stereotactic body radiotherapy of lung as measured by Aoki *et al* with an exponent function $\exp(-t)$. (a) Clinical data for largest tumor cross-section; (b) approximation of clinical data to tumor volume.

The fitting of the exponential function was done using the least-squares minimization based on a version of a quasi-Newton method called the L-BFGB-B algorithm (Byrd *et al* 1995). This code is widely used in the medical physics community for solving different radiotherapy optimization problems of different complexity (Chvetsov *et al* 2007). The mathematical function which has been used for the fitting has been presented as a weighted linear combination of an exponent function and a constant function

$$f(t) = (1 - w)\exp(-\mu_0 t) + w, \tag{7}$$

where w is a constant value between 0.0 and 1.0. This has been done to subtract the constant saturation value in the clinical data during the optimization process.

The results of the fitting are shown in figure 2 for adenocarcinoma and in figure 3 for SCC. We have obtained the average value of half-life $T_{1/2} = 28.2$ days and standard deviation $\sigma = 8.6$ days for SCC and the average value of half-life $T_{1/2} = 72.4$ days and standard

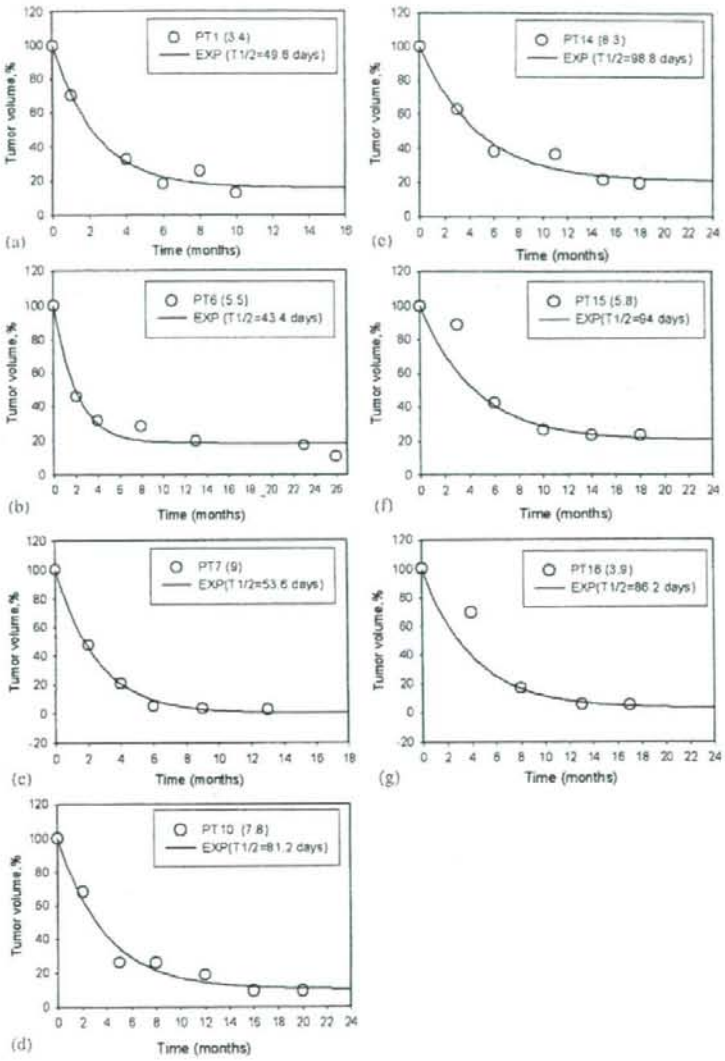

Figure 2. Comparison of the lung adenocarcinoma volume after stereotactic body radiotherapy in clinical data of Aoki *et al* with the function $(1-w)\exp(-\ln 2t/T_{1/2})+w$: (a)–(g) patients 1–7. Tumor size (cm^2) is shown for each patient in parentheses.

deviation $\sigma = 22.8$ days for adenocarcinoma. Assuming that the potential doubling time T_{pot} is 7.7 days for adenocarcinoma and 8.5 days for SCC according to the data published by Shibamoto and Hara (2005), we obtain the average value of the disintegration parameter $b = 9.4$ for adenocarcinoma and $b = 3.3$ for SCC. These data indicate that an adenocarcinoma cell cycling approximately three times longer after lethal radiation damage than a SCC cell before it disintegrates. Using the half-life we can also evaluate the mean life of a single cell if